Journal of the Oceanographical Society of Japan
Vol. 38, pp. 172 to 182, 1982

Origin of the *Abiki* Phenomenon (a Kind of Seiche) in Nagasaki Bay*

Toshiyuki HIBIYA** and Kinjiro KAJIURA**

Abstract: Large oscillations of water level in Nagasaki Bay are called *Abiki* and are most frequently observed in winter. The largest *Abiki* recorded in the past 20 years at the tide station at Nagasaki occurred on March 31, 1979. Simultaneously, a distinct atmospheric pressure disturbance of solitary type with an amplitude of about 3 mb was recorded at several neighbouring stations in Kyûshû, which indicated the pressure disturbance probably travelled eastward with an average speed of about 110 km h^{-1}.

The quantitative relation between this pressure disturbance and notable seiches observed in Nagasaki Bay is examined by means of numerical simulation, and it is confirmed that the exceptionally large range of oscillations in the bay, which reached 278 cm at the tide station, was indeed produced by this travelling pressure disturbance.

The leading part of shallow water waves induced by the atmospheric pressure disturbance was amplified up to about 10 cm in amplitude, over the broad continental shelf region off China, because of near resonant coupling to the pressure disturbance. After leaving this continental shelf region, the amplified water wave converged into the shelf region (Gotô Nada) surrounded by the north-western coast of Kyûshû and the Gotô Islands and excited eigenoscillations on the shelf. A train of waves thus formed with a period of about 35 min entered Nagasaki Bay and was resonantly amplified at periods of 36 min and 23 min which are the eigen periods of the bay. Besides resonance, the combined effects of shoaling and reflection inside Nagasaki Bay also enhanced the amplification.

1. Introduction

Large seiches in Nagasaki Bay called *Abiki* are noted for their extraordinary amplitudes and frequent occurrence, particularly in winter (TERADA *et al.*, 1953; NAKANO & UNOKI, 1962; AKAMATSU, 1978). Sometimes, strong currents induced by notable seiches cause severe damage to cargo-vessels and fishing boats by tearing their mooring lines. Partly from the necessity to avoid such accidents, detailed studies have been made of this phenomenon both theoretically and experimentally by TERADA *et al.* (1953). They clarified possible modes of oscillation in Nagasaki Bay by analysis of observed tide-gauge records together with some theoretical considerations, and also by use of a hydraulic model experiment. ISHIGURO and FUJIKI (1955) investigated the response of Nagasaki Bay when complex external forces were given at the mouth of the bay by using an electric analogue network which simulated the hydraulic system of Nagasaki Bay. As a result of these investigations, the oscillatory characteristics of water in Nagasaki Bay are now well understood.

Using another approach, some statistical studies on the occurrence of *Abiki* at Nagasaki in relation to synoptic patterns of weather-maps were made by TERADA *et al.* (1953) and AKAMATSU (1978) who pointed out that the occurrence of *Abiki* is almost always accompanied by a sudden change of atmospheric pressure recorded on barograms not only at Nagasaki but also at Tomié in the Gotô Islands located to the west of mainland Kyûshû. Therefore, it has been speculated that long-period oceanic waves induced by travelling pressure disturbances in Gotô Nada (the Sea of Gotô: see Fig. 10) excite the seiches of large amplitude in Naga-

* Received Nov. 25, 1981, revised Apr. 14 and accepted June 2, 1982.

** Earthquake Research Institute, University of Tokyo, 1-1-1 Yayoi, Bunkyô-ku, Tokyo 113, Japan

saki Bay.

The problem of coupling between moving air-pressure disturbances and sea level variations was discussed long ago (see PROUDMAN, 1952: pp. 295 -300) and, in particular, PLATZMAN (1958) succeeded in the numerical simulation of the surge of 26 June 1954 on Lake Michigan caused by an intense and fast-moving squal-line. Therefore, the basic understanding of air-sea coupling of this type is now established, and the problems to be clarified for *Abiki* phenomenon in Nagasaki Bay are: 1) To find a quantitative relation between the travelling atmospheric pressure disturbance and the generated water waves including the excitation of seiches in Nagasaki Bay, is it possible to explain the very large range of seiches in Nagasaki Bay in terms of air-sea coupling due to the observed pressure disturbances?; and 2) To understand the nature of observed atmospheric pressure disturbances, how and where the atmospheric pressure disturbance is generated and how the disturbance propagates. A way to predict *Abiki* phenomena may be successfully contemplated on the basis of understanding of the above. In the present study, the first problem is studied by taking the large oscillations in Nagasaki Bay observed on March 31, 1979 at the Nagasaki tide station as an example. The quantitative relation between the travelling atmospheric pressure disturbance, a model of which is assumed on the basis of available barogram records, and notable seiches in Nagasaki Bay is explored by means of numerical simulation. At the same time, the mechanisms of amplification of water waves which occur at various stages during the course of their propagation are clarified.

2. Observations

Nagasaki Bay is a narrow and long bay, connected with the open ocean through its mouth which opens to the west (see Fig. 1). The characteristic length and width of the bay are about 6 km and 1 km respectively and the average depth is 20 m. The tide station at Nagasaki is located about halfway along the inner bay. In the afternoon of March 31, 1979, a notable seiche was observed in the bay. Figure 2 shows the tide-gauge record at that time. After a few oscillations beginning at 12: 10 JST the maximum range (crest to trough

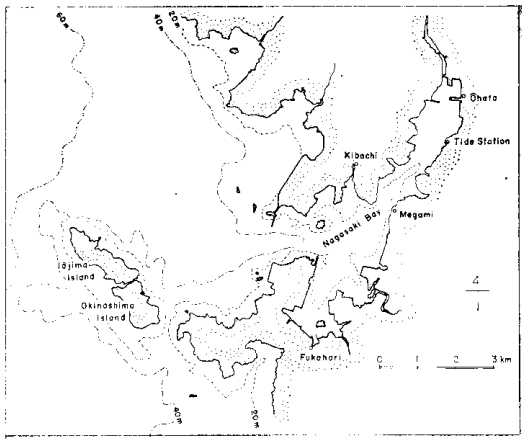

Fig. 1. Map of Nagasaki Bay.

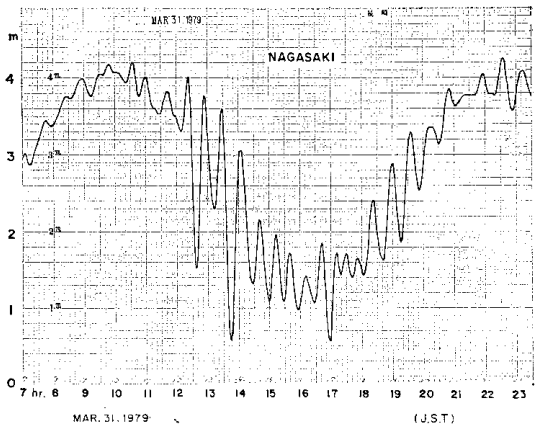

Fig. 2. The tide-gauge record at Nagasaki on March 31, 1979.

height) of 278 cm was reached at about 13:30. Notable seiches also occurred at various other locations in Kyûshû and it was reported that three elderly women were drowned on account of the sudden and unexpected rise of sea level at Tamanoura in the Gotô Islands.

Shortly after the first significant water wave was recorded on the tide-gauge at Nagasaki, a remarkable atmospheric pressure change of solitary type was observed at the weather station at Nagasaki although no particular changes of weather conditions were recognized. Similar pressure changes were also recorded at Fukué, Meshima Island, Ushibuka and other places in Kyûshû.

Barograph records obtained at Meshima Island, Fukué and Nagasaki are shown in Fig. 3 (for the geographical locations of these stations,

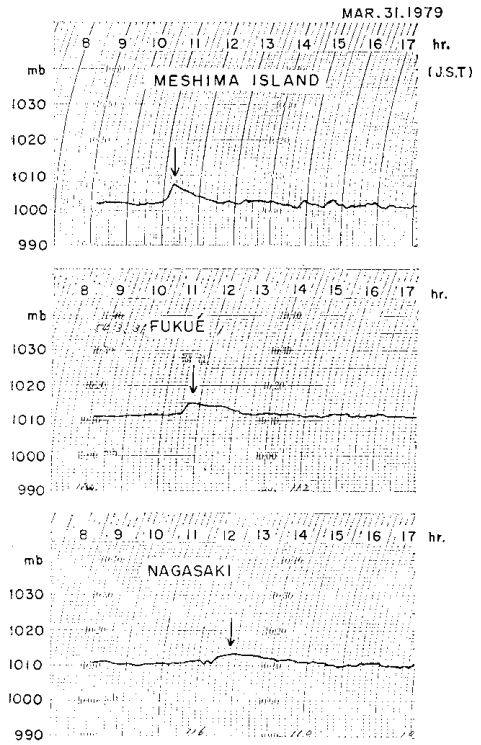

Fig. 3. Barograms of an atmospheric pressure wave on March 31, 1979.

see Fig. 5). As is typically seen on the record at Meshima Island, the pressure change began with a rapid increase in pressure for about 15 min followed by a gradual decrease to the previous pressure level in about 90 min. The magnitude of the pressure jump was 2 to 6 mb depending on the station. Our understanding of this type of atmospheric pressure disturbances is still unsatisfactory and no quantitative study to explain its generation and behaviour in the East China Sea is available. However, if we assume the pressure disturbance propagates in the form of a line front and the phases indicated by arrows for three stations in Fig. 3 to represent the same feature, the possible propagation velocity of the pressure wave is estimated to be 1.88 km min^{-1} (about 110 km h^{-1}) in the direction of 5.6 degrees north of east. Indeed, successive cloud images taken on the same day by the geostationary meteorological sattelite *Himawari* operated by the Japan Meteorological Agency indicate a distinctive cloud pattern moving from the Chinese mainland to Kyûshû over the East China Sea with a velocity roughly equal to that estimated here. Therefore, we may assume that the pressure wave also travelled across the East China Sea at this speed.

3. Numerical simulation

a) Formulation

The linearized, depth-integrated shallow water equations for an inviscid fluid are used for a numerical simulation study, because our interest is in the barotropic response of the ocean to the atmospheric pressure disturbance the horizontal extent of which is quite large compared to the ocean depth.

Let x, y denote horizontal cartesian coordinates directed to the east and south respectively and z the vertical coordinate directed upward with the origin at the undisturbed sea surface. In this coordinate system, shallow water equations of motion and continuity can be written as

$$\frac{\partial Q_x}{\partial t} = -gh \cdot \frac{\partial}{\partial x}(\eta - \eta^*) \tag{1}$$

$$\frac{\partial Q_y}{\partial t} = -gh \cdot \frac{\partial}{\partial y}(\eta - \eta^*) \tag{2}$$

and

$$\frac{\partial \eta}{\partial t} = -\left(\frac{\partial Q_x}{\partial x} + \frac{\partial Q_y}{\partial y}\right) \tag{3}$$

where h is the depth of the sea, Q_x and Q_y are the depth-integrated transport components in the directions of x and y, respectively, η is the water surface elevation relative to the still water level and $\eta^* = -p/(\rho \cdot g)$ where p is the atmospheric pressure deviation at the sea surface, g is the acceleration due to gravity and ρ is the mean density of sea water.

In the above formulation, the Coriolis force due to the earth's rotation is neglected because the period of waves considered here is much less than the inertial period, and the frictional forces are also neglected because the generated wave remains in a wide sea region most of the time and also we are concerned only with a transient phenomenon of relatively short duration. In addition, the wind stress term is omitted compared with the total pressure gradient force, because the observed wind velocity was low and did not change appreciably both before and after the pressure wave had passed each weather station.

Using square grids with spacing Δs in horizontal space and applying the centered difference and leap-frog scheme with a time increment Δt, (1) to (3) can be replaced by a finite difference scheme and the spatial distribution of η and those of Q_x and Q_y can be computed alternately with suitable initial and boundary conditions. Here the water transport is calculated at the center of the line connecting two successive grid points and the water surface elevation at the center of four neighbouring grid points. The atmospheric pressure (represented by η^*) is also specified at the same place as η (Fig. 4). The depth corresponding to each grid point is read from hydrographic charts and adjusted relative to the mean sea level near the coast.

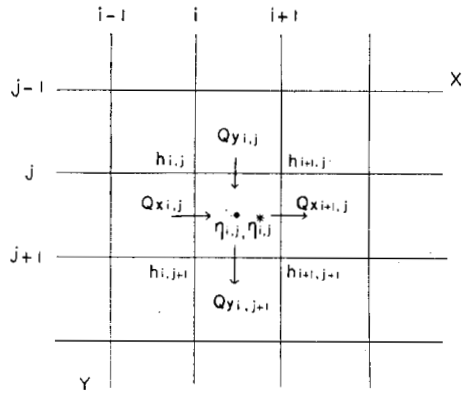

Fig. 4. Schematization of the finite difference grid.

The domain of the calculation is shown in Fig. 5. The grid interval Δs is 4 km in Region I and 2 km in Region II. Furthermore, regions in the vicinity of tide stations of interest, Nagasaki and Fukué in the Gotô Islands, are divided into finer meshes in order to calculate the wave forms accurately: the grid intervals are successively decreased to 1 km, 500 m, 250 m and 125 m on approach to each tide station and η, Q_x and Q_y are linearly interpolated at the junction of two different grid intervals (see AIDA, 1974). Taking the stability condition of numerical calculation into account, Δt is chosen to be 0.05 min.

b) A model of the atmospheric pressure wave

A model of the air-pressure disturbance applied here is shown in Fig. 6. Assuming the

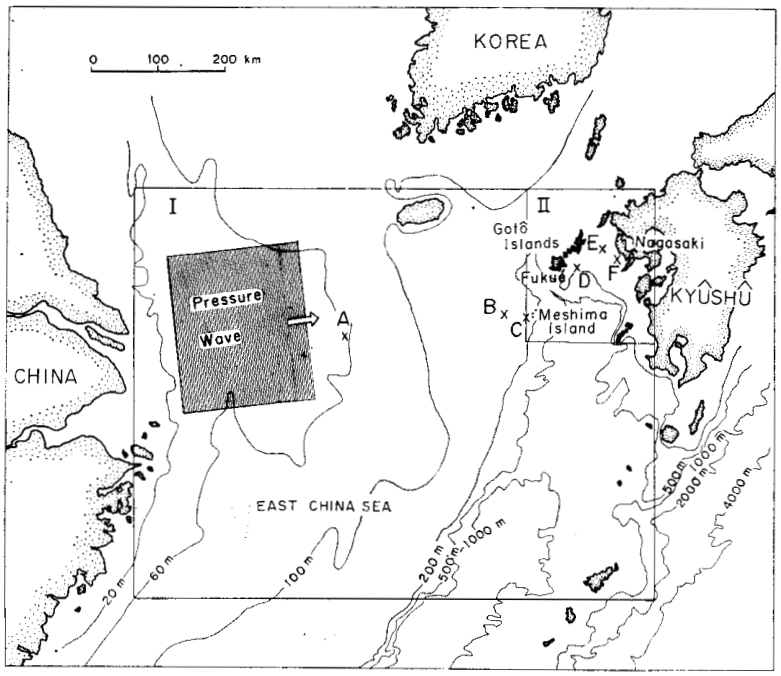

Fig. 5. Domain of the numerical computation. The grid interval is 4 km in Region I, and 2 km in Region II. The shaded area indicates the assumed initial location of the pressure wave.

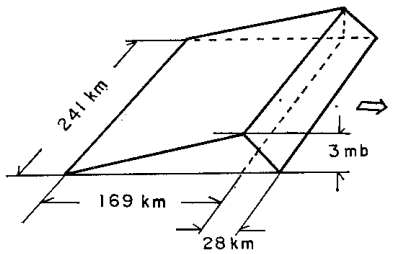

Fig. 6. Schematic view of the pressure wave model. The direction of propagation is indicated by the arrow.

propagation velocity v of this pressure wave to be 1.88 km min^{-1}, the numerical values relevant to this model are determined as follows: within the region of the pressure wave, the atmospheric pressure increases linearly from the front to the crest by $\Delta p=3$ mb in a distance of L_1 (=28 km) and returns to its previous level, also linearly, in a distance of L_2 (=169 km) from the crest rearwards with no lateral gradient within its assumed width of 241 km. The width of 241 km was determined by examining the distribution of pressure jump intensities recorded at various weather stations in Kyûshû. This width might be too small, but we have no definite information on the lateral extent of this pressure wave. Since we are ignorant of the behaviour of the atmospheric pressure wave in the East China Sea, we assume the pressure wave modelled above occurs instantaneously in the shaded region in Fig. 5 at $t=0$ (the front of which is located about 246 km east of the Chinese mainland). Furthermore, the model disturbance is assumed to propagate in the direction indicated by the arrow (5.6 degrees north of east) with a constant velocity of propagation of 1.88 km min^{-1} without change of shape.

Although these pressure wave parameters might involve considerable uncertainty, the result of numerical simulation is scarcely changed even if we change the values of parameters by, say, 10 percent of the assigned values.

c) Initial and boundary conditions

Initital conditions are that the ocean is at rest (Q_x, $Q_y=0$ and $\eta=0$) at $t=0$. The coast assumed to be a rigid vertical wall with perfect reflection. An approximate radiation boundary condition is applied on open boundaries to allow waves to escape from the region of concern. For this purpose, the relation between the water surface elevation and the transport of plane progressive waves is applied on these open boundaries. For example, along a boundary parallel to the y-axis, Q_x is computed by

$$Q_x=\pm\left\{(gh)\cdot\eta^2-Q_y^2\right\}^{1/2} \qquad (4)$$

where the sign of Q_x is selected so that the water flows out from the region of calculations when η is positive.

4. Results

Calculated sea level variations at the tide stations at Nagasaki and Fukué are shown respectively in Fig. 7a and b by the solid lines while the observed ones after eliminating ordinary tides are indicated by the broken lines. The agreement between the calculated and observed oscillations at Nagasaki is close both in amplitude and phase. The maximum range of sea level variations takes place at the third

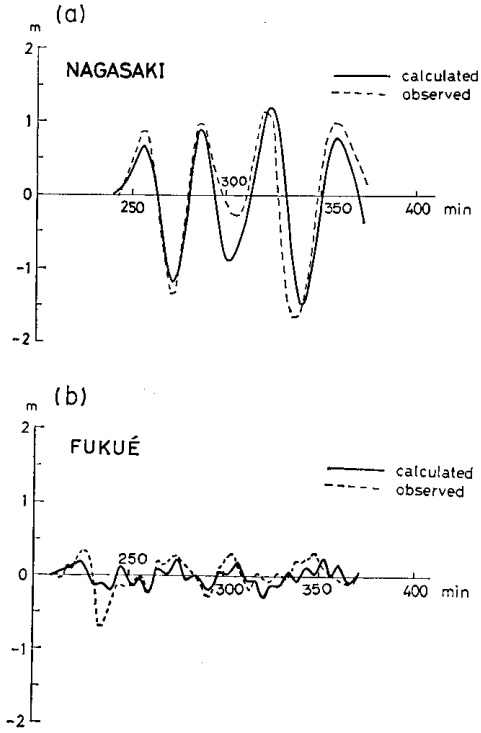

Fig. 7. Simulated sea level variations (solid lines) at the tide stations at Nagasaki (a) and Fukué (b). Observed ones are shown by broken lines.

oscillation in both the observed and simulated records. The agreement of the calculated pattern of sea level variations at Fukué with the observed one is not so good, but general characteristics of the oscillations are considered to be simulated well, though high frequency components exist in the simulated water level variations.

It is now clear that the conspicuous seiches with their maximum range of 278 cm, which occurred on March 31, 1979, at the Nagasaki tide station can be explained by the observed travelling pressure wave with an amplitude of about 3 mb, provided that the pressure disturbance is assumed to propagate over the East China Sea with a velocity of about 110 km h^{-1}. Thus, it is interesting to explore how the long-period water wave, induced in the East China Sea by the pressure disturbance, is amplified as it propagates toward the coast of Kyûshû and excites large seiches in Nagasaki Bay.

5. Discussion

a) Amplification of water waves on the continental shelf off China

A shallow continental shelf in the East China Sea extends eastward for about 600 km from the Chinese mainland. Over most of the shelf, the depth is about 50 to 150 m. The velocity of shallow water waves propagating in this region, therefore, is about 1.3 to 2.3 km min^{-1} and is comparable to that of the assumed atmospheric pressure wave which is 1.88 km min^{-1}. Thus, efficient coupling between the atmospheric pressure wave and the generated shallow water wave may be expected to occur.

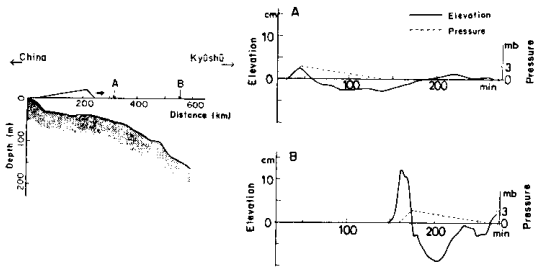

Fig. 8. Typical profile of the continental shelf off China in the direction of pressue wave propagation (left figure); and the calculated sea level time-variations at Locations A and B (see Fig. 5) — two points selected along the propagation direction of the pressure wave (right figure).

Results of the present simulation at Locations A and B (see Fig. 5) are shown in Fig. 8. The maximum elevation at Location A is only 2 cm but it increases to about 12 cm at Location B, which is located about 550 km from the continental boundary and about 300 km from the initial location of the front of the assumed pressure wave. As seen in the wave patterns at both locations, a trough of long duration following the first sharp crest is the typical wave pattern generated by the transient forcing of the solitary-type pressure disturbance. At Location B, the front of the water wave appears ahead of the forcing, because $c>v$ in this region where $c^2=gh$, and after the first crest, a deep trough follows with a secondary hump in the trough which is seen at about 230 min. These features are partly due to the effect of the finite lateral extent of the forcing region.

It is well known, in the case of one-dimensional propagation in the x-direction, that the pure forced wave $\eta_f(x-vt)$ with the phase velocity v in water of constant depth, generated by a travelling atmospheric pressure disturbance with the velocity v of the form $\eta^*(x-vt)$ is given by $\eta_f=\eta^*/(1-v^2/c^2)$. Thus, the forced water wave η_f is in phase with η^* if $v<c$ and out of phase if $v>c$. When c approaches v, resonance makes η_f formally infinite. However, in the vicinity of resonance condition $v=c$, we have to treat the problem as an initial value problem, in which the amplitude of the water wave increases linearly with time t. For the same atmospheric pressure model as in the simulation study, the maximum elevation $\Delta\eta$ of water level can be computed easily by the method of characteristics. In contrast to the case of a pure forced wave, the maximum appears in the front part of the forcing region, $x_f=vt$, and is given by

$$\Delta\eta=-(\Delta\eta^*/L_1)\cdot x_f/2 \qquad (5)$$

where x_f is the distance travelled by the front, $\Delta\eta^*=-\Delta p/(\rho\cdot g)$ where Δp is the pressure amplitude and L_1 is the distance from the pressure maximum to the front. Thus, if we take $L_1=30$ km and $x_f=300$ km, the amplification factor $|\Delta\eta/\Delta\eta^*|$ is about 5 and if $\Delta\eta^*=-3$ cm, as is assumed in the present case, $\Delta\eta$ would reach

about 15 cm. It is interesting to note that the resonant amplification is inversely proportional to L_1 so that a rapid increase in atmospheric pressure is essential for a large amplification factor at a fixed distance x_f. In the numerical simulation, $\Delta\eta$ at Location B is 12 cm and the amplification is somewhat smaller, because in the realistic case the depth of water increases gradually from the continental boundary to the edge of the shelf and the exact conditions of resonance cannot be met over a large part of the shelf.

A more realistic situation is examined for the case of one-dimensional propagation by taking the realistic depth change of the East China Sea into account. For the same initial condition as in the case of numerical simulation, the maximum water level elevation at Location B is numerically computed for different propagation velocities of the atmospheric disturbance. The results are shown in Fig. 9, where we can see that the optimum speed of atmospheric forcing for this bottom topography is about 1.5 km min^{-1} to 1.8 km min^{-1} with a maximum amplification of the water waves by a factor of 4.3. This result indicates that the assumed speed of 1.88 km min^{-1} for the atmospheric forcing is near the optimum for resonant amplification.

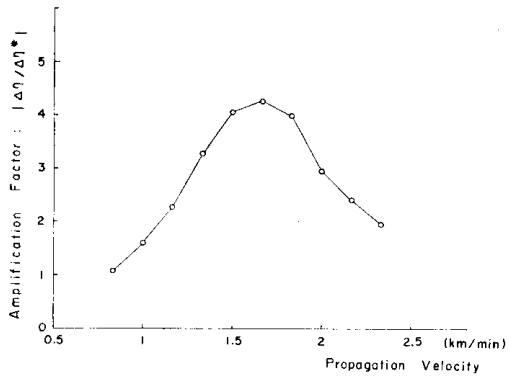

Fig. 9. The amplification factor of water wave height at Location B (see Fig. 5) for various propagation velocities of the atmospheric pressure wave (one-dimensional model).

b) Transformation in Gotô Nada

Between Locations C and D, shallow shelves are separated by a deep trough (see Fig. 5), so that the leading water wave moves ahead of the forcing region as a free gravity wave. As seen in Fig. 10, the direction of propagation of the first wave crest is gradually turned to the north by the refractive effects of bottom topography and is almost normally incident in the shelf region (Gotô Nada) between the mainland of Kyûshû and the Gotô Islands. Possibly because of the combined effects of refraction, reflection and shoaling, the elevation of the first wave crest in this region does not change appreciably and is about 12 cm at Location F where the depth is about 100 m. However, the following trough which is very distinct in the wave signature at Location B does not show up clearly because of the interference of the incoming wave trough with the reflected wave from the shelf slope and the coastlines of mainland Kyûshû and the Gotô Islands.

The excitation of natural oscillations in Gotô Nada can be noticed in the power spectra of simulated water level variations at several locations (D, E and F) in Gotô Nada. In Fig. 11, the eigen-oscillations with periods of 70, 36 and 24 mins are present. The mode with longer

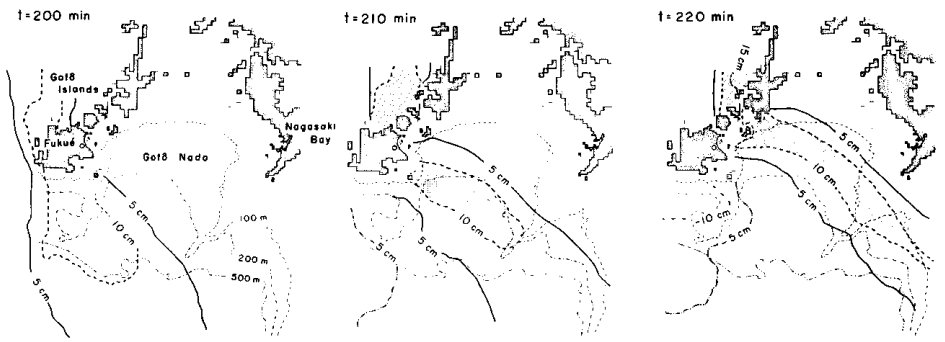

Fig. 10. Patterns of the propagation into Gotô Nada of the first water wave crest (shaded area). Numerals on the contours represent the water surface elevation.

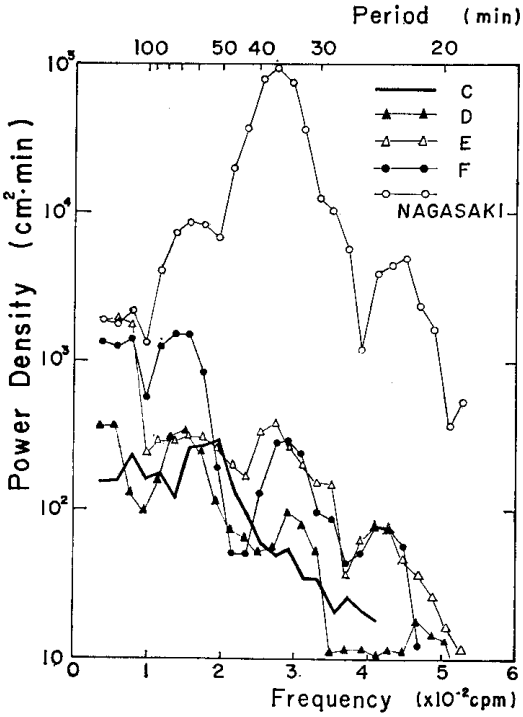

Fig. 11. Power spectra of simulated water level variations at Locations C, D, E, F (see Fig. 5) and at the Nagasaki tide station.

periods, if it exists, cannot be resolved adequately because spectra are computed from simulated data up until only 512 min from the onset of oscillations. In the same figure, the power spectrum of incident waves at Location C is also shown for comparison, which exhibits no distinct peak at periods shorter than about 50 min. To determine the characteristics of natural oscillations in Gotô Nada more definitely, the eigen-value problem is solved numerically and it is found that the fundamental mode in Gotô Nada has a period of 171 min which is the shelf oscillation with a node located offshore of the shelf slope. Higher modes with periods of 64, 36 and 24 mins are lateral oscillations with nodes running more or less in the north-south direction, suggesting that the waves reflected at the coasts of the Gotô Islands and mainland Kyûshû form an oscillating system.

c) Amplification in Nagasaki Bay

As is evident in Fig. 11, the level of the power spectrum at Nagasaki relative to those in Gotô Nada is very high and mean power amplification in the period range shorter than about 50 min amounts to 40. Superimposed on this mean amplification, the amplification due to resonance is noted at the periods of about 36 min and 23 min, which are not only the eigen-periods of Gotô Nada but also coincide with the periods of oscillations in Nagasaki Bay with the nodes in the vicinity of the bay mouth and at the constriction near Megami (see Fig. 1), respectively.

To understand the mechanism of this large amplification, let us consider two factors: one is the amplification of progressive waves as they proceed toward the head of the bay due to topographic convergence effects and the other is the effect of dynamic resonance.

The wave signature at Location G (see Fig. 13) located outside Nagasaki Bay where the depth is 60 m is shown in Fig. 12, where the simulated first crest height is about 20 cm and the duration of a positive elevation is about 20 min. However, if we formally separate the water surface elevation into "incoming" and "outgoing" one-dimensional waves by taking information on time variations of transport into account, it is found that the first crest is already affected by the interference between the "incoming" and "outgoing" waves, and the first crest height A_G of the "incoming" wave is about 16 cm (see Fig. 12). The increase of the apparent first crest height as well as that of the "incoming" waves as they approach the head of Nagasaki Bay is shown in Fig. 13, in which amplification obeying Green's law is also shown for reference with the height adjusted to the "incoming" wave crest height outside the bay mouth, at Location H. The total topogra-

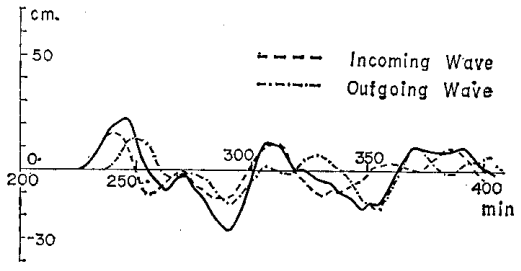

Fig. 12. Calculated sea level variations (solid line) at Location G (see Fig. 13), along with the time histories of "incoming" (dashed line) and "outgoing" (dash and dot line) waves at the same location.

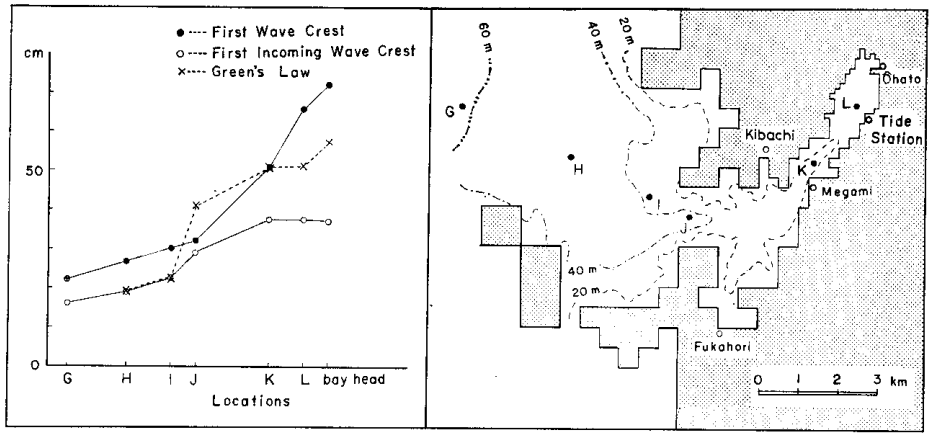

Fig. 13. Calculated first crest heights of water waves at several locations selected along the bay-axis (locations are indicated in the map on the right). The first crest heights of "incoming" waves separated from "outgoing" waves are also plotted, along with those estimated by Green's formula, assuming both are equal in height outside the bay mouth at Location H.

phic amplification, A_L/A_G, of the "incoming" wave from Locations G to L is 38/16. The "incoming" wave height at the bay head may be approximated by A_L, since in the inner bay the "incoming" wave height does not change significantly. The increase of the "incoming" wave crest height is dictated by the combined effects of topographic convergence inside the bay and partial reflection at the bay mouth in the vicinity of Location J and at the constriction near Location K.

Now, the resonant effect of the fundamental mode in one-dimensional waves can be evaluated as follows. By the incidence of a uniform train of waves with the resonant frequency ω_0, wave energy is accumulated in the bay by total reflection at the head and partial reflection at the mouth of the bay. The final resonant amplitude B_{max} at the head of the bay is given by

$$B_{max}/(2A)=1/(1-|R|) \qquad (6)$$

where A is the "incoming" wave amplitude at the location of the bay head without the effect of resonance and $|R|$ is the absolute value of the reflection coefficient at the mouth of the bay. It is easily shown that a nearly resonant amplitude (90 percent of the stationary amplitude) is attained only after, say, $(-2 \log |R|)^{-1}$ cycles from the start of oscillations.

In terms of α, the ratio of the admittance in the bay side to that in the outer channel side at the junction at Location J, the reflection coefficient R is expressed as

$$R=(1-\alpha)/(1+\alpha) \qquad (7)$$

and the relative band width $\Delta\omega$ between the half points of the power spectrum near resonance at the bay head is given by

$$\Delta\omega/\omega_0 \sim 4 \cdot \alpha/\pi \qquad (8)$$

The quality factor Q of the oscillating system with radiation damping is approximately given by $\pi/(4 \cdot \alpha)$ (see KAJIURA, 1966).

Although no detailed analysis is made on the radiation damping of Nagasaki Bay, it is reasonable to assume $\alpha=0.2$ for the fundamental mode, since $\Delta\omega/\omega_0 \simeq 0.7/2.75$ in Fig. 11. Then, it follows $R=0.667$, and the Q factor is about 4. The amplification due to resonance becomes

$$B_{max}/(2A) \simeq 3.0 \qquad (9)$$

and this saturation amplitude is attained only after 2 to 3 wave cycles. Since the topographic amplification of incident waves from Locations G to L is 38/16, we may roughly estimate the resonant amplitude at the head of the bay relative to the mean amplitude of the "incoming" wave train at Location G to be $(38/16)\times 3\times 2 = 14.25$. If we follow the conventional defini-

tion of wave amplification by taking the wave height instead of amplitude for "incoming" waves at Location G, the amplification factor is about 7.

Returnig to the time history of the incident waves at Location G shown in Fig. 12, a wave train with a period of about 35 min is recognized in the early stages. A small second wave crest is identified as being caused by the atmospheric pressure forcing which took place mainly in the shallow shelf region of Gotô Nada after the first wave crest moved ahead of the forcing region as a free gravity wave. The origin of the "incoming" third wave crest which lags by about 70 min from the first crest is not clear, but it seems to be the reflection of the first "incoming" wave at the coasts of the mainland Kyûshû and again at the coasts of the Gotô Islands. This view may be supported by the fact that 64 min is the period of natural oscillation in Gotô Nada with only one nodal line running north-south, and in Fig. 12, oscillation with this period is very distinct.

The mean amplitude of these first oscillations at a period of about 35 min is estimated to be, say, 10 cm at Location G, so that the resonant amplitude at the bay head after 3 cycles of incident waves is about $10 \times 14.25 \simeq 140$(cm). The total range would be about 280 cm which is very close to that actually observed.

6. Conclusion

A quantitative relation between the travelling atmospheric pressure disturbance and notable seiches in Nagasaki Bay, which occurred on March 31, 1979, is examined by means of numerical simulation, and it is confirmed that the conspicuous seiches which had a maximum range of 278 cm at the tide station at Nagasaki can be explained quantitatively by the effects of the observed travelling pressure wave which had an amplitude of about 3 mb.

A shallow water wave generated on the continental shelf off China by the atmospheric pressure disturbance was amplified at various stages of propagation:

(1) The leading part of the shallow water waves with a time scale of about 20 min is amplified on the broad continental shelf off China by up to about 4 times the inverted barometric elevation of the water surface by near resonant coupling to the travelling pressure disturbance.

(2) The height (double amplitude) of the "incoming" water wave which is about 20 cm is amplified by a factor of about 2.4 between the outer sea (depth 60 m) and the head of Nagasaki Bay due to the combined effects of partial reflection and shoaling inside the bay even without the effects of resonance.

(3) Resonant amplification in Nagasaki Bay due to the incoming of a train of successive waves formed by the direct forcing of the atmospheric pressure wave and reflection and refraction in Gotô Nada adds a further amplification factor of about 3.

Thus, the maximum amplification at the head of Nagasaki Bay becomes 7 times the mean height (double amplitude) of an incoming wave train in the outer sea with a period of about 35 min.

Needless to say, the present study is concerned with only one case of the *Abiki* phenomenon and there is the possibility that large seiches along the west coast of Kyûshû might be produced by other types of pressure waves. Further investigation into the characteristics of atmospheric pressure waves is desirable to obtain a complete picture of the *Abiki* phenomenon, the prediction of which will be possible in the future through the combination of observations of water waves and atmospheric pressure waves preferably on the continental shelf region in the East China Sea, with detailed studies of the response characteristics of various locations along the west coast of Kyûshû.

Acknowledgements

The authors express their thanks to Messrs. M. OKADA and H. AKAMATSU of the Japan Meteorological Agency, and Dr. H. NITANI of the Japan Maritime Safety Agency for their help in collecting data.

References

AIDA, I. (1974): Numerical computation of a tsunami based on a fault origin model of an earthquake. J. Seismol. Soc. Japan, Ser. II, **27**, 141–154 (in Japanese).

AKAMATSU, H. (1978): *Abiki* Phenomenon in Nagasaki Harbour. *In*, 100th Anniversary Volume of the Nagasaki Marine Observatory, ed. and published by the Nagasaki Marine Observatory, Naga-

saki, pp. 154-162 (in Japanese).
ISHIGURO, S. and A. FUJIKI (1955): An analytical method for the oscillation of water in a bay or lake, using an electric network and an electronic analogue computer. J. Oceanogr. Soc. Japan, **11**, 191-197.
KAJIURA, K. (1966): Tsunami. Hydraulic Engineering Series 66-13, ed. by the Comittee on Hydraulics of the Japan Soc. Civil Engrs, JSCE, Tokyo, pp. 1-22 (in Japanese).
NAKANO, M. and S. UNOKI (1962): On the seiches (the secondary undulations of tides) along the coasts of Japan. Records Oceanogr. Works Japan, Special No. (6), 169-214.
PLATZMAN, G. W. (1958): A numerical computation of the surge of 26 June 1954 on Lake Michigan. Geophysica, **6**, 407-438.
PROUDMAN, J. (1952): Dynamical Oceanography: Methuen, London, 409 pp.
TERADA, K., Z. YASUI and S. ISHIGURO (1953): On the secondary undulations in Nagasaki Harbour. The Report of the Nagasaki Marine Observatory, (4), 1-73 (in Japanese).

長崎湾におけるあびき現象(湾内の大規模なセイシュ)の発生機構

日比谷 紀 之*, 梶 浦 欣二郎*

要旨: 長崎湾内で通例は冬期にしばしば見られるあびきが，1979年3月31日に長崎海洋気象台観測史上最大の規模で発生した．これを例として，数値シミュレーションを行ない，その発生機構について，定量的な考察を試みた．その結果，湾内の顕著な振動（長崎験潮所で最大潮位差278 cmを記録）は，東シナ海を，ほぼ東向きに，約110 km h^{-1} の速度で進行した振幅約3 mbの気圧波によっておこされたとすれば説明できることがわかった．また，その発生の過程については，

1) 東シナ海大陸棚上での気圧波との共鳴的カップリングによる海洋長波の振幅10 cmに及ぶ増幅；2) 長崎湾内での浅水増幅および反射干渉による増幅；3) 長崎湾の固有振動系と，五島灘領域の振動系との干渉による共鳴増幅効果など，数段階の増幅作用が絡んでおり，これらによって生成された約35分周期の一連の波によって，同湾の固有周期に相当する36分および23分周期で共鳴的に増幅されたことが，定量的に結論づけられた．

* 東京大学地震研究所 津波・高潮部門
〒113 東京都文京区弥生 1-1-1